The optimal stack spacing for thermoacoustic refrigeration

Article *in* The Journal of the Acoustical Society of America · August 2002

DOI: 10.1121/1.1487842 · Source: PubMed

3 authors, including:

M.E.H. Tijani
TNO
37 PUBLICATIONS **899** CITATIONS
SEE PROFILE

Alphons De Waele
Eindhoven University of Technology
126 PUBLICATIONS **2,120** CITATIONS
SEE PROFILE

The optimal stack spacing for thermoacoustic refrigeration

M. E. H. Tijani,[a] J. C. H. Zeegers, and A. T. A. M. de Waele
Department of Applied Physics, Eindhoven University of Technology, P.O. Box 513, 5600 MB Eindhoven, The Netherlands

(Received 28 November 2001; revised 19 April 2002; accepted 25 April 2002)

The characteristic pore dimension in the stack is an important parameter in the design of thermoacoustic refrigerators. A quantitative experimental investigation into the effect of the pore dimensions on the performance of thermoacoustic devices is reported. Parallel-plate stacks with a plate spacing varying between 0.15 and 0.7 mm are manufactured and measured. The performance measurements show that a plate spacing in the stack of 0.25 mm ($2.5\delta_k$) is optimum for the cooling power. A spacing of 0.4 mm ($4\delta_k$) leads to the lowest temperature. The optimum spacing for the performance is about 0.3 mm ($3\delta_k$). It is concluded that a plate spacing in the stack of about three times the penetration depth should be optimal ($3\delta_k$) for thermoacoustic refrigeration. © *2002 Acoustical Society of America.* [DOI: 10.1121/1.1487842]

PACS numbers: 43.35.Ud, 43.35.Ty [RR]

I. INTRODUCTION

Thermoacoustic refrigerators are devices which use sound to generate cooling power. They consist mainly of an acoustic resonator filled with a gas. In the resonator a stack consisting of a number of parallel plates and two heat exchangers are installed, as shown in Fig. 1. A loudspeaker generates a standing wave in the resonance tube. The thermal interaction of the oscillating gas with the surface of the stack generates a heat transfer from one end of the stack to the other end. The heat exchangers are necessary to exchange heat with the surroundings, at the cold and hot sides of the stack. The way these systems work is explained extensively in the literature.[1,2]

The stack forms the heart of the refrigerator where the heat-pumping process takes place, and it is thus an important element which determines the performance of the refrigerator. A detailed experimental study of the effect of the plate spacing in the stack on the performance of thermoacoustic systems is still lacking in the literature. In this paper the result of a systematic investigation into the effect of the spacing in the stack on the behavior of the refrigerator is reported. Stacks with plate spacing varying between 0.15 and 0.7 mm have been constructed and measured. The manufacturing technique along with the measurement results are described in the following.

II. STACK MATERIAL AND GEOMETRY

The heat conductivity through the stack material and gas in the stack region has a negative effect on the performance of thermoacoustic refrigerators.[1,3] The stack material must have a low thermal conductivity and a heat capacity much larger than the heat capacity of the working gas in order that the temperature of the stack plates remains steady. The material Mylar is chosen, as it has a low heat conductivity (0.16 W/mK) and is proposed in thicknesses of 10–500 μm.

There are many geometries which the stack can have: parallel plates, circular pores, pin arrays, triangular pores, etc. The geometry of the stack is expressed in Rott's function f_k.[4] As can be seen from the energy equation, the cooling power is proportional to $\mathrm{Im}(-f_k)$.[4,5] Figure 2 shows the real and imaginary parts of f_k for some geometries as functions of the ratio the hydraulic radius r_h and the thermal penetration depth. The pin arrays and parallel-plate stacks are the most effective geometries. Since the pin-array stack is too difficult to manufacture, it is decided to use a stack made of parallel plates. Figure 3 shows an illustration of a parallel-plate stack. We note that for parallel-plate stack $r_h = y_0$.

The selection of an operating frequency of 400 Hz, an average pressure of 10 bar, and helium as working gas, determines the thermal and viscous penetration depths given by, respectively,

$$\delta_k = \sqrt{\frac{2K}{\rho c_p \omega}}, \tag{1}$$

and

$$\delta_\nu = \sqrt{\frac{2\mu}{\rho\omega}}, \tag{2}$$

where K is the thermal conductivity of the gas, μ is the viscosity of the gas, ρ is the density of the gas, c_p is the isobaric specific heat per unit mass, and ω is the angular frequency of the sound wave. Using Eqs. (1) and (2) for our system we have $\delta_k = 1$ mm and $\delta_\nu = 0.08$ mm.

As can be seen from Fig. 2 for a parallel-plate stack $\mathrm{Im}(-f_k)$ has a maximum for $y_0/\delta_k = 1.1$. Since the spacing in the stack is $2y_0$, this means that the theoretical optimal spacing is about 0.22 mm ($2.2\delta_k$). Using an analogous analysis, Arnott *et al.*[5] showed an optimal spacing of about 0.26 mm. In order not to alter the acoustic field, it was stated[2] to use a spacing of $2\delta_k$ to $4\delta_k$. It is decided to investigate experimentally the effect of the spacing in the stack by constructing parallel-plate stacks with spacings varying between 0.15 and 0.7 mm.

[a]Electronic mail: m.e.h.tijani@tue.nl

 0001-4966/2002/112(1)/128/6/$19.00

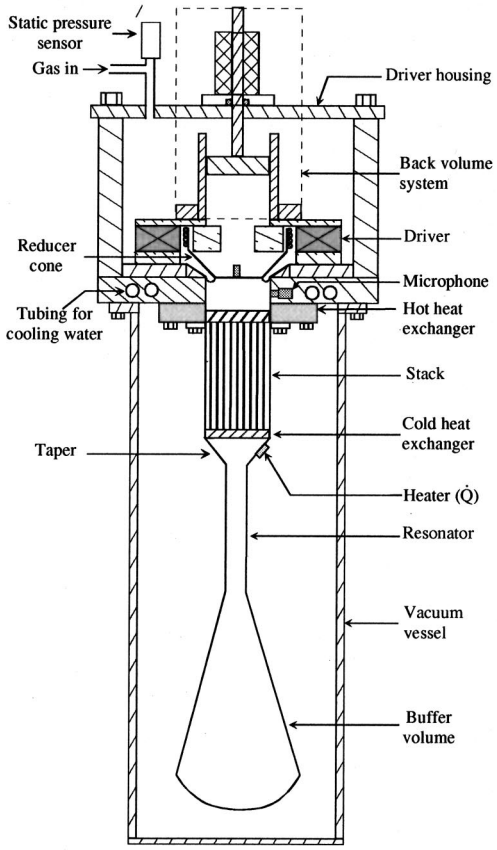

FIG. 1. Cross-sectional illustration of the thermoacoustic refrigerator, showing the different parts.

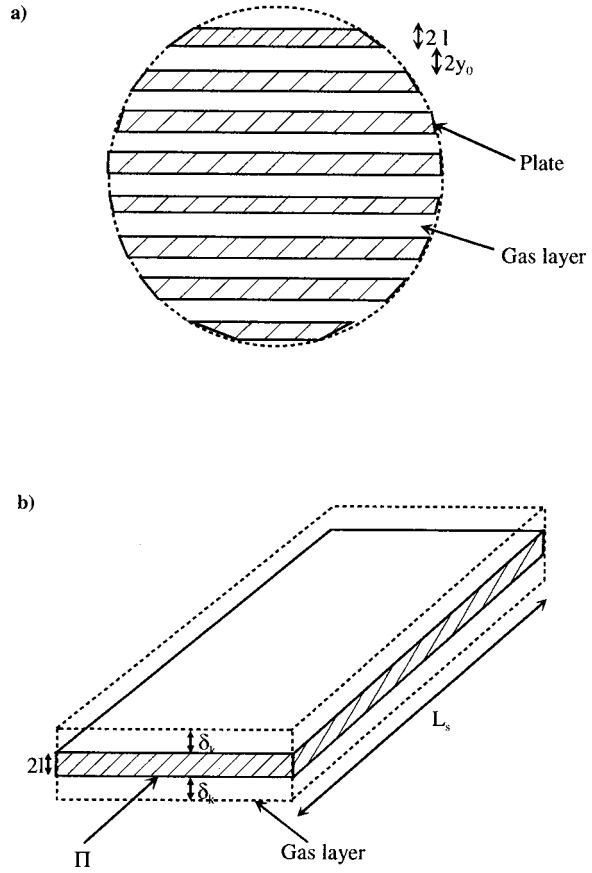

FIG. 3. Illustration of a parallel-plate stack. (a) Cross-sectional view of the stack, the plates are $2l$ thick and are $2y_0$ spaced. (b) A plate of the stack is shown.

III. MANUFACTURING OF THE PARALLEL-PLATE STACKS

The parallel-plate stacks consist of parallel plates which are spaced by fishing line spacers glued between the plates, as shown in Fig. 4(b). This type of stack is more difficult to manufacture than the spiral stack which one rolled up, results in a rigid structure.[6,7] In parallel-plate stacks the adhesion between the plates is ensured by the spacers which provide only a small adhesion surface. This leads to a fragile structure. One of the manufacturing problems to overcome was the gluing of nylon fishing line onto Mylar plates. Good results are obtained with 3M Scotch-Grip 7312 glue.[3]

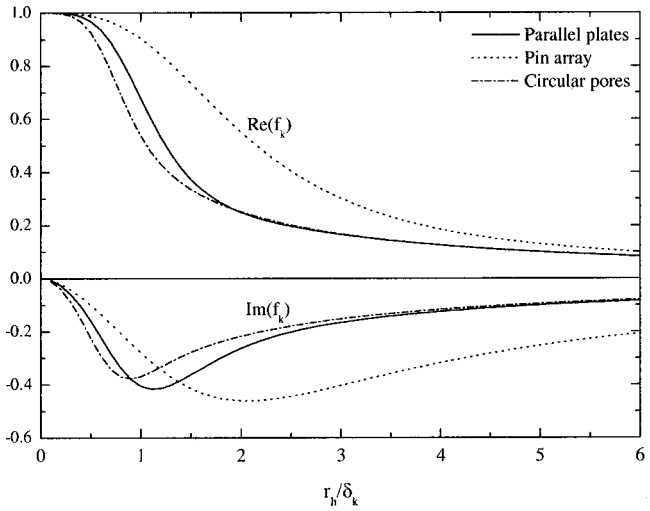

FIG. 2. Imaginary and real parts of the Rott function f_k as function of the ratio of the hydraulic radius and the thermal penetration depth. Three geometries are considered. The pin arrays and parallel-plate stacks are the best. The pin arrays an internal radius $r_i = 3\delta_k$ is used in the calculations.

For ease and speed of construction a special mounting setup was built, as shown in Fig. 4(a). The setup consists of a work plate which supports vertical rods. The diameter of the rods can be varied, depending on the spacing between the plates. Since fishing lines with different diameters are used to realize different stacks with different spacings, the number of rods is increased as the diameter becomes smaller. This increase in the number of rods is needed to obtain a uniform channel structure and enough surface for adhesion.

A fishing reel is mounted on a vertical bar. This reel is used to provide the needed tension on the fishing line during the winding process. A plastic syringe is used as a reservoir for glue as well as handle to stretch the line. The manufacturing procedure of the parallel plate stacks is as follows. The 0.1-mm-thick Mylar plates are first cut to the needed dimensions. A plate is placed between the brass rods as shown in Fig. 4(a). The fishing line enters the syringe from the top hole, through the glue and exits the syringe via the bottom hole. The latter has a little oversized diameter so that the thickness of the film of glue on the fishing line is 0.15 mm. In this way a uniform film of glue is obtained on the line. The fishing line is first wound around the first aluminum rod, and then around the brass rods [Fig. 4(a)]. At the end of

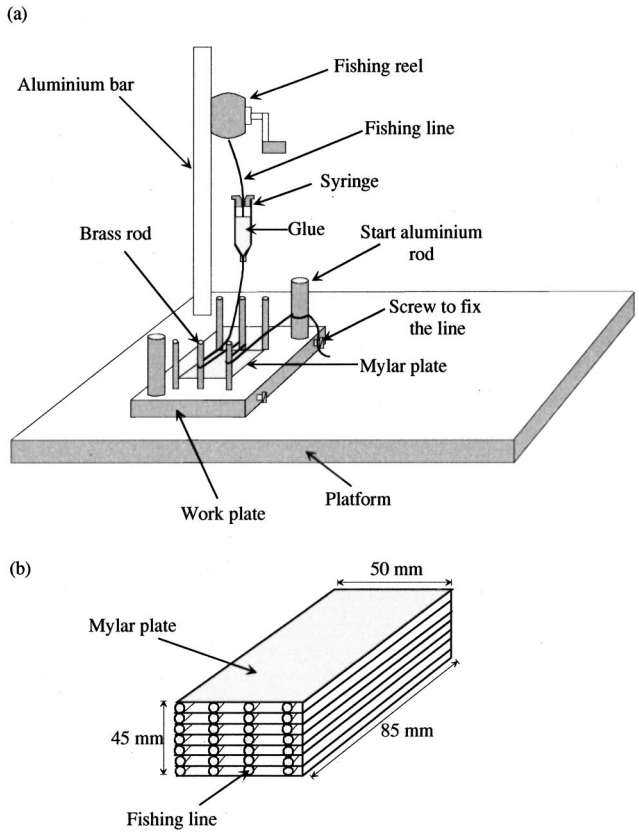

FIG. 4. Illustration of the manufacturing technique of the parallel-plate stack. A plate is placed between the brass rods, then the glue coated fishing line coming from the syringe is would around the rods to get parallel strings. The strings are then pressed onto the plate and another plate may be placed. The procedure is repeated until the needed height of the stack is reached. (a) Setup. (b) A parallel-plate stack as released from the work plate.

the winding process the line is wound around the last aluminum rod and fixed by a screw to the edge of the work plate. A press (stamper) is used to affix the fishing lines to the plate. Then, a new plate is placed on the strings and the winding process starts again. This stacking procedure is repeated until the needed height of the stack is obtained. The stack is pressed by a stainless steel block and the glue is allowed to dry for at least one day. The stack is then shaped into a cylindrical form of diameter 38 mm, using a milling technique. The building of a stack takes one day, and the shaping process two days. We note that care was taken during the winding process so that just enough tension is used, otherwise the stack will be deformed. In total seven stacks have been successfully manufactured with a spacing varying between 0.15 and 0.7 mm. It should be noted that all of the stacks have the same diameter, the same length, the same plate thickness, and are placed at the same location in the resonator.

IV. EXPERIMENTAL SETUP

An illustration of the thermoacoustic refrigerator used for the measurements is shown in Fig. 1. A modified loudspeaker (driver) is attached to one end of an acoustic resonator which is filled with helium gas at 10 bar. A stack and two heat exchangers are placed in the resonator. The loudspeaker sustains an acoustic standing wave in the gas, at the fundamental resonance frequency of the resonator. The other end of the resonator terminates in a buffer volume which simulates an open end. The system is essentially a quarter-wavelength system, with a pressure antinode at the loudspeaker end and pressure node at the buffer volume end. The acoustic driver consists of a modified moving-coil loudspeaker, from which the fabric dome was cut off near the voice coil and replaced by a thin walled light aluminum cone glued onto the voice coil. A rolling diaphragm is used to seal the resonator from the driver housing, as shown in Fig. 1. A detailed description of the setup can be found elsewhere.[3,8,9]

The stack is mounted in a stack holder which is made out of POM-Ertacetal, a material with high rigidity and low thermal conductivity. The holder has an inner diameter of 38 mm, a wall thickness of 2 mm, and a length of 85 mm. It has two flanges for connections to the cold and hot heat exchanger flange. The holder is connected to the flange of the hot heat exchanger via six bolts. As this junction is at room temperature a rubber O-ring, mounted into the flange of the hot heat exchanger, is used for sealing. At the cold heat exchanger side, the stack holder is attached to the tapered part via twelve bolts. Because this side cools to below $-40\,^{\circ}\mathrm{C}$, we used an indium O-ring to seal this junction. Different stacks can be interchanged easily so that different performance measurements can be carried out.

The duty of a refrigerator is to remove a heat quantity ($\dot{Q}_C$) at a low temperature (T_C) and to supply a heat quantity ($\dot{Q}_H$) to the surroundings at a high temperature (T_H). To accomplish this process a net work input ($\dot{W}$) is required. The performance of the refrigerator, called the coefficient of performance (COP), is defined as

$$\mathrm{COP}=\frac{\dot{Q}_C}{\dot{W}}. \tag{3}$$

The Carnot coefficient of performance is defined as

$$\mathrm{COPC}=\frac{T_C}{T_H-T_C}. \tag{4}$$

This forms the maximum performance for all refrigerators, where T_H is the temperature of the hot heat exchanger, and T_C is the temperature of the cold heat exchanger. The coefficient of performance relative to Carnot's coefficient of performance is defined as

$$\mathrm{COPR}=\frac{\mathrm{COP}}{\mathrm{COPC}}. \tag{5}$$

The performance measurements for the refrigerator are presented in plots of COP, COPR, and ΔT given by

$$\Delta T=T_C-T_H, \tag{6}$$

as functions of the total heat load. To understand the behavior of the cooler as a function of the varied parameters, the measured ΔT data will be fit with

$$\Delta T=\Delta T_0+\alpha\dot{Q}, \tag{7}$$

where $\dot{Q}$ is the total heat load which is the sum of the heat applied by the heater to the cold heat exchanger and the

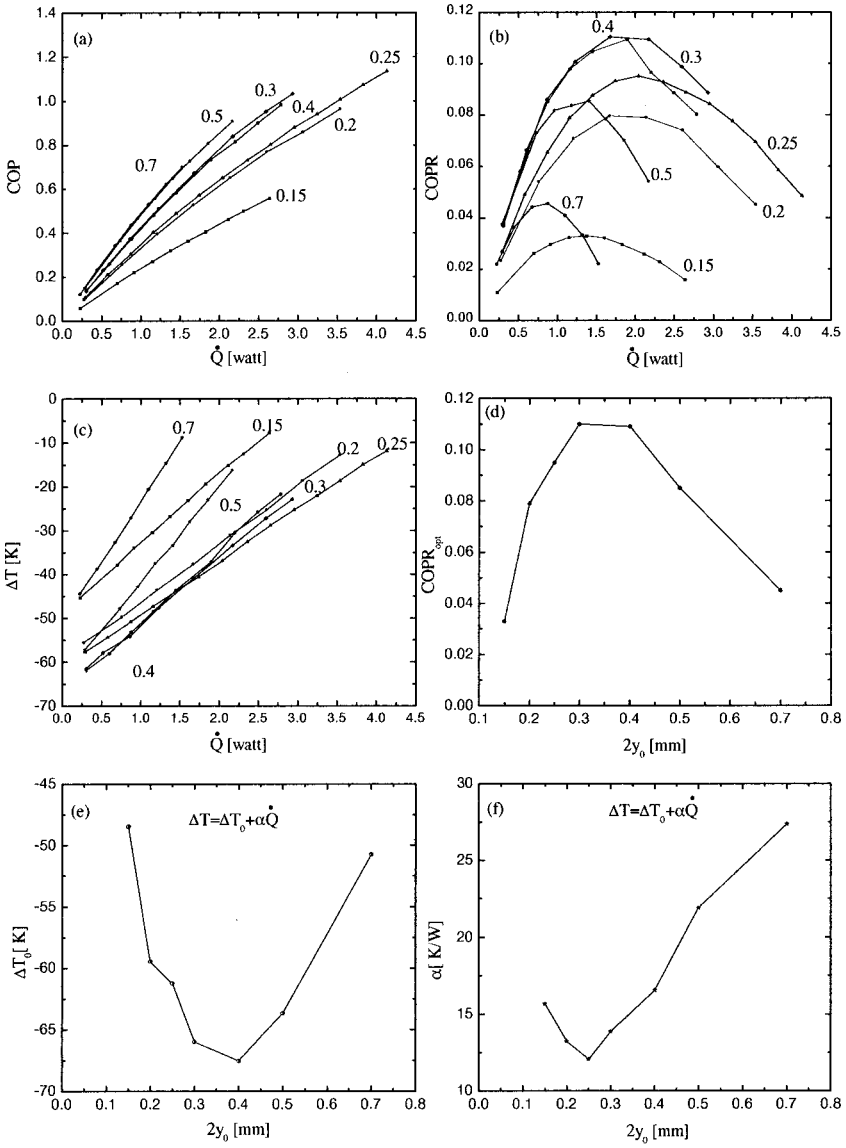

FIG. 5. Measurements with different stacks having plate spacing between 0.15 and 0.7 mm. The working gas is helium at 10 bar, and the drive ratio is 1.4%. In (a), (b), and (c) the values of the spacing $2y_0$ are indicated at the corresponding curves. (a) COP. (b) COPR. (c) ΔT. (d) Optimal COPR corresponding to the peak COPR as function of $2y_0$. (e) ΔT_0 as function of $2y_0$. (f) α as function of $2y_0$.

external heat leak.[3] During a given performance measurement the drive ratio, defined as the ratio of the dynamic pressure to the average pressure, is held constant while stepwise the heat load is increased and the temperature is allowed to stabilize. The heat load is applied by an electric heater which is placed at the cold heat exchanger. Two thermometers are used to monitor the temperature at the hot heat exchanger, and the cold heat exchanger. The thermometers are read by a multimeter which in turn is read by a computer. For all measurements and DELTAE[10] calculations reported in this paper, helium at an average pressure of 10 bar is used as working gas. A drive ratio $D=p_1/p_m=1.4\%$ is also used, where p_m is the average pressure and p_1 is the dynamic pressure.

V. RESULTS AND DISCUSSION

Performance measurements have been done with different stacks, having a plate spacing, $2y_0$, which varies between 0.15 and 0.7 mm. Figure 5 shows the measurements results. As can be seen from Fig. 5(a), the COP increases as function of the heat load for all stacks. Additionally, the slope of COP is an increasing function of $2y_0$. The COPR shows a parabolic behavior with a maximum [Fig. 5(b)] for all stacks, but the magnitude and the position of the peak changes as the spacing changes. To get a better insight into the effect of the spacing on COPR, the maxima from Fig. 5(b) are plotted as function of $2y_0$ in Fig. 5(d). The COPR shows a maximum at a spacing of about 0.3 mm ($3\delta_k$).

The temperature differences as functions of the heat load and the spacing are shown in Fig. 5(c). For all stacks, the dependence on the heat load is linear but again the slope changes as the spacing changes. For a better illustration of the influence of the spacing on the temperature difference, the curves in Fig. 5(c) are fitted with Eq. (7). Figure 5(e) shows that the temperature difference without heat load, ΔT_0, has an optimum around a plate spacing of about 0.4 mm ($4\delta_k$), which we did not expect. On the other hand, Fig. 5(f) shows that the coefficient α has an optimum at a plate spacing of about 0.25 mm ($2.5\delta_k$). Since a minimum for α leads to a maximum for the cooling power, the experimental optimal spacing is in agreement with the theoretical expectation.

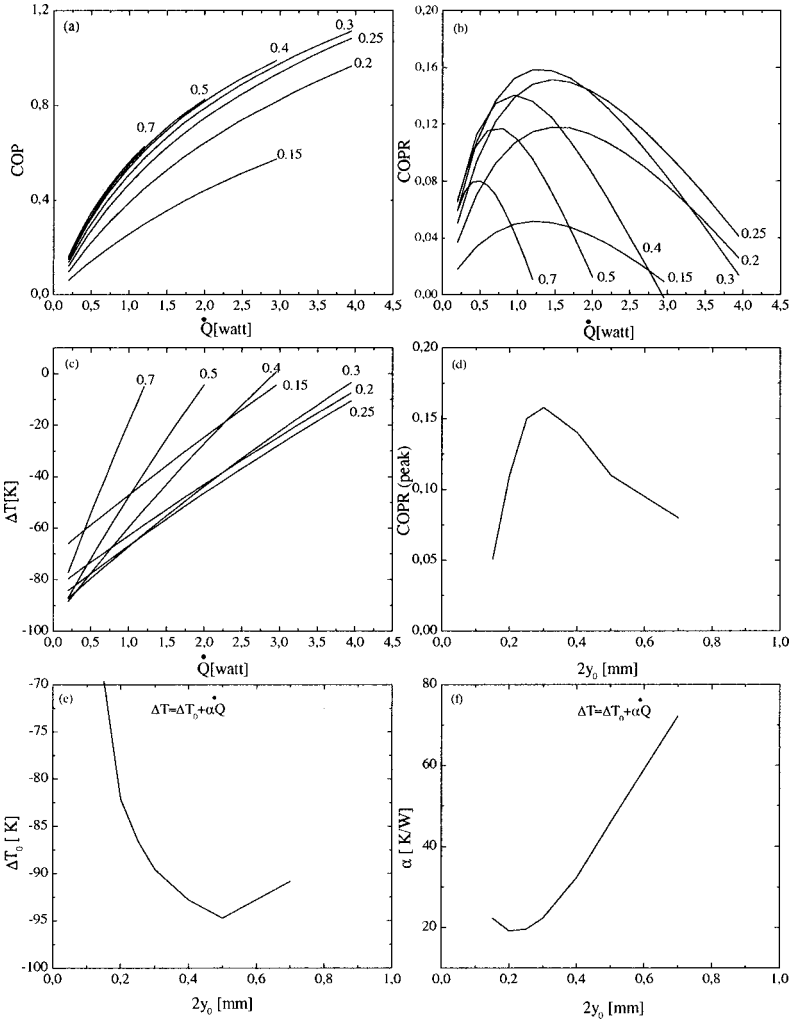

FIG. 6. DELTAE calculations with different stacks having plate spacing between 0.15 and 0.7 mm. The working gas is helium at 10 bar and the drive ratio is 1.4%.

The behavior of the cooling power (α) and COPR can be explained as follows: For plate spacings larger than about $2\delta_k$, the boundary layer picture holds and the cooling power is proportional to the product of the total perimeter of the stack in the cross section (Π) and the thermal penetration depth δ_k[1] (Fig. 3). An increase in the spacing means a decrease of the number of plates and hence a decrease of the perimeter. This results in a decrease of the cooling power and COPR above around $3\delta_k$. On the other hand, once the spacing becomes smaller than about $2.5\delta_k$, the thermoacoustic shuttle effect will be reduced, which will decrease the cooling power. Additionally, the whole gas layer between the plates contributes to the viscous shear and the small spacing induces higher velocities and hence extra viscous losses. This explains the rapid decreasing of COPR for spacings smaller than about $3\delta_k$. Since for the stacks having smaller spacing more fishing lines are used to keep the plates parallel and to obtain a uniform channel structure, this has as effect to change the geometry from parallel plate toward rectangular channel, which is less efficient. This may also contribute to the rapid decrease of the performance below about $3\delta_k$. It should be noted that the porosity of the stack, i.e., the ratio of the gas area to the total area in the cross section, varies from 87% for the stack with a plate spacing of 0.7 mm to 60% for the stack with a plate spacing of 0.15 mm.

The above-discussed apply to the stack position and length used in our refrigerator which are obtained from the optimization procedure used to design our refrigerator.[3,8,9] The effect of the stack position on the above-discussed optima will be discussed in Sec. VI, which is concerned with DELTAE calculations.

VI. DELTAE CALCULATIONS

The simulation program DELTAE[10] has been used to predict the performance of the refrigerator. DELTAE is a computer program which resolves the thermoacoustic linear equations in a geometry given by the user. As it is a linear tool, the nonlinearities, which may occur in practice, are not included. The calculations for the different stacks are shown in Fig. 6. The general trend is in agreement with the measurements. Figure 6(b) shows the behavior of the COPR as a function of the heat load and for different stacks. Both the magnitude and position of the peak are influenced by the stack spacing. In Fig. 6(d), $\mathrm{COPR}_{\mathrm{opt}}$ is plotted versus the plate spacing in the stack. The $\mathrm{COPR}_{\mathrm{opt}}$ shows a maximum around 0.3 mm, which is in agreement with the measurements. The ΔT curves shown in Fig. 6(b) are fitted with Eq. (7). The coefficients ΔT_0 and α are plotted versus the plate spacing in Figs. 6(e) and (f), respectively. The coefficient α shows an optimum around 0.22 mm in agreement with the measurements [Fig. 6(f)]. The parameter ΔT_0 shows an op-

timum around 0.5 mm. It should be noted that the calculated ΔT curves are not exactly linear. This may explain the discrepancy between the experimental and calculated optima for ΔT_0. In summary, the calculations show a general trend which is in agreement with the measurements.

Because the experiments are lengthy and time consuming and seeing the good agreement between experiment and DELTAE calculations, we decided to simulate the effect of the stack position on the above-discussed optima using DELTAE. The calculations show that the optimal spacing for the cooling power (α) is nearly independent of the position of the stack in the acoustic field, and that the optimal spacing for COPR shifts to lower spacings as the position of the stack decreases (position zero corresponds to the driver location). This is due to the decrease of the velocity which results in a decrease of the viscous losses and hence an increase of the performance.

VII. CONCLUSION

The influence of the plate spacing in the stack on the behavior of the refrigerator was studied systematically. The performance of the thermoacoustic refrigerator, using stacks with plate spacings varying between 0.15 and 0.7 mm, is measured. We showed using a simplified analytical discussion that the parallel plate geometry is the best, and that a sheet spacing in the stack of about $2.5\delta_k$ should be optimal for the cooling power. As can be seen from Figs. 5(b) and (f), the cooling power for the stacks with a spacing of $2.5\delta_k$ and $3\delta_k$ are nearly equal. Additionally, the stack with the spacing of $3\delta_k$ has the highest performance. Taking into account this remark it is safe to say that the practical optimal spacing in the stack is about $3\delta_k$. This result is also confirmed by DELTAE calculations. The general trend of the DELTAE calculations show a satisfactory agreement with experiment.

ACKNOWLEDGMENTS

The authors would like to thank Greg Swift and Chris Espinoza of Los Alamos National Laboratories for their advice in the engineering of the parallel-plate stacks.

[1] G. W. Swift, ''Thermoacoustic engines,'' J. Acoust. Soc. Am. **84**, 1146–1180 (1988).
[2] J. C. Wheatley, T. Hofler, G. W. Swift, and A. Migliori, ''An intrinsically irreversible thermoacoustic heat engine,'' J. Acoust. Soc. Am. **74**, 153–170 (1983); ''Experiments with an intrinsically irreversible thermoacoustic heat engine,'' Phys. Rev. Lett. **50**, 499–502 (1983).
[3] M. E. H. Tijani, ''Loudspeaker-driven thermo-acoustic refrigeration,'' Ph.D. thesis, unpublished, Eindhoven University of Technology, 2001.
[4] G. W. Swift, ''Thermoacoustic engines and refrigerators,'' *Encyclopedia of Applied Physics*, edited by G. L. Trigg (Wiley-VCH, Verlag, Berlin, 1997), Vol. 21, pp. 245–264.
[5] W. P. Arnott, H. E. Bass, and R. Raspet, ''General formulation of thermoacoustics for stacks having arbitrarily shaped pore cross sections,'' J. Acoust. Soc. Am. **90**, 3228–3237 (1991).
[6] S. L. Garrett, J. A. Adeff, and T. J. Hofler, ''Thermoacoustic refrigerator for space applications,'' J. Thermophys. Heat Transfer **7**, 595–599 (1993).
[7] T. J. Hofler, ''Thermalization refrigerator design and performance,'' Ph.D. dissertation, Physics Department, University of California at San Diego, 1986.
[8] M. E. H. Tijani, J. C. H. Zeegers, and A. T. A. M. de Waele, ''Design of thermoacoustic refrigerators,'' Cryogenics **42**, 49–57 (2002).
[9] M. E. H. Tijani, J. C. H. Zeegers, and A. T. A. M. de Waele, ''Construction and performance of a thermoacoustic refrigerator,'' Cryogenics **43**, 59–66 (2002).
[10] W. C. Ward and G. W. Swift, ''Design environment for low-amplitude thermoacoustic engines,'' J. Acoust. Soc. Am. **95**, 3671–3672 (1994).